

# Potent Vasoconstrictor Kisspeptin-10 Induces Atherosclerotic Plaque Progression and Instability: Reversal by its Receptor GPR54 Antagonist

Kengo Sato, PhD;\* Remina Shirai, MSc;\* Mina Hontani, BSc; Rina Shinooka, BSc; Akinori Hasegawa, MSc; Tomoki Kichise, BSc; Tomoyuki Yamashita, BSc; Hayami Yoshizawa, MSc; Rena Watanabe, MSc; Taka-aki Matsuyama, MD, PhD; Hatsue Ishibashi-Ueda, MD, PhD; Shinji Koba, MD, PhD; Youichi Kobayashi, MD, PhD; Tsutomu Hirano, MD, PhD; Takuya Watanabe, MD, PhD

**Background**—Kisspeptin-10 (KP-10), a potent vasoconstrictor and inhibitor of angiogenesis, and its receptor, GPR54, have currently received much attention in relation to pre-eclampsia. However, it still remains unknown whether KP-10 could affect atherogenesis.

**Methods and Results**—We evaluated the effects of KP-10 on human umbilical vein endothelial cells, human monocyte-derived macrophages, human aortic smooth muscle cells in vitro, and atherosclerotic lesions in apolipoprotein E-deficient (ApoE<sup>-/-</sup>) mice in vivo. KP-10 significantly increased the adhesion of human monocytes to human umbilical vein endothelial cells, which was significantly inhibited by pretreatment with P234, a GPR54 antagonist. KP-10 stimulated mRNA expression of tumor necrosis factor- $\alpha$ , interleukin-6, monocyte chemoattractant protein-1, intercellular adhesion molecule-1, vascular adhesion molecule-1, and E-selectin in human umbilical vein endothelial cells. KP-10 significantly enhanced oxidized low-density lipoprotein-induced foam cell formation associated with upregulation of CD36 and acyl-CoA:cholesterol acyltransferase-1 in human monocyte-derived macrophages. In human aortic smooth muscle cells, KP-10 significantly suppressed angiotensin II-induced migration and proliferation, but enhanced apoptosis and activities of matrix metalloproteinase (MMP)-2 and MMP-9 by upregulation of extracellular signal-regulated kinase 1 and 2, p38, Bcl-2-associated X protein, and caspase-3. Four-week-infusion of KP-10 into ApoE<sup>-/-</sup> mice significantly accelerated the development of aortic atherosclerotic lesions with increased monocyte/macrophage infiltration and vascular inflammation as well as decreased intraplaque vascular smooth muscle cells contents. Proatherosclerotic effects of endogenous and exogenous KP-10 were completely canceled by P234 infusion in ApoE<sup>-/-</sup> mice.

**Conclusions**—Our results suggest that KP-10 may contribute to accelerate the progression and instability of atheromatous plaques, leading to plaque rupture. The GPR54 antagonist may be useful for prevention and treatment of atherosclerosis. Thus, the KP-10/GPR54 system may serve as a novel therapeutic target for atherosclerotic diseases. (*J Am Heart Assoc.* 2017;6:e005790. DOI: 10.1161/JAHA.117.005790.)

**Key Words:** atherosclerosis • endothelial cell • kisspeptin-10 • macrophage • plaque instability • smooth muscle cell • vasoconstriction

**K**isspeptins (KPs) are biologically active cleavage peptides encoded by the *KiSS1*. The *KiSS1* gene encodes a 145-amino-acid protein, which is enzymatically cleaved into a

54-amino-acid peptide, KP-54, and shortened peptides of 14, 13, or 10 amino acids.<sup>1,2</sup> KPs activate a G-protein-coupled receptor, GPR54 (KiSS1R).<sup>1,3,4</sup> *KiSS1* suppresses metastases

From the Laboratory of Cardiovascular Medicine, Tokyo University of Pharmacy and Life Sciences, Tokyo, Japan (K.S., R. Shirai, M.H., R. Shinooka, A.H., T.K., T.Y., H.Y., R.W., T.W.); Department of Pathology, National Cerebral and Cardiovascular Center, Osaka, Japan (T.M., H.I.-U.); Division of Cardiology, Department of Medicine (S.K., Y.K.) and Division of Diabetes, Metabolism, and Endocrinology (T.H.), Showa University School of Medicine, Tokyo, Japan.

Accompanying Data S1 and Figures S1, S2 are available at <http://jaha.ahajournals.org/content/6/4/e005790/DC1/embed/inline-supplementary-material-1.pdf>

\*Dr Sato and Dr Shirai contributed equally to this work.

This work was presented, in part, at the American Heart Association Scientific Sessions, November 7–11, 2015, in Orlando, FL, and at the 65th Annual Scientific Session of the American College of Cardiology, April 2–4, 2016, in Chicago, IL.

**Correspondence to:** Kengo Sato, PhD, Laboratory of Cardiovascular Medicine, Tokyo University of Pharmacy and Life Sciences, 1432-1 Horinouchi, Hachioji-City, Tokyo 192-0392, Japan. E-mail: ksato@toyaku.ac.jp

Received February 13, 2017; accepted March 8, 2017.

© 2017 The Authors. Published on behalf of the American Heart Association, Inc., by Wiley. This is an open access article under the terms of the Creative Commons Attribution-NonCommercial License, which permits use, distribution and reproduction in any medium, provided the original work is properly cited and is not used for commercial purposes.

of human melanoma and breast carcinoma.<sup>5,6</sup> Its gene product, KP-54 (also known as metastin), inhibits metastases of melanoma and breast cancer cells.<sup>1,7</sup> The common C-terminal decapeptide shared by these KPs, KP-10, is the minimum sequence necessary for GPR54 activation<sup>1,3,4</sup> and is secreted by cultured human trophoblasts.<sup>8</sup> KP-10 is highly conserved between mice and humans, with only 1 amino acid replacement.<sup>9</sup> KP-10 is well known as the most potent activator of gonadotropic hormone secretion<sup>10</sup> and also exerts potent vasoconstriction, antitumor angiogenesis, and anticoagulation.<sup>11–14</sup> KP-10 inhibits the migration of human umbilical vein endothelial cells (HUVECs) and subsequent angiogenesis through inhibition of vascular endothelial growth factor signaling.<sup>15,16</sup> KP-10 induces the senescence and suppresses the proliferation in HUVECs.<sup>17</sup> Both KPs and GPR54 have been identified in human aorta, coronary artery, and umbilical vein.<sup>11</sup> Recently, KPs have generated much interest in relation to pre-eclampsia.<sup>18</sup> However, there have been no previous reports regarding the roles of the KP-10/GPR54 system in atherogenesis.

Atherosclerosis is a chronic inflammatory response to injury of the arterial wall.<sup>19</sup> Endothelial inflammation stimulates the production of proatherogenic adhesion molecules, such as tumor necrosis factor- $\alpha$  (TNF- $\alpha$ ), interleukin-6 (IL-6), monocyte chemoattractant protein-1 (MCP-1), intercellular adhesion molecule-1 (ICAM-1), vascular adhesion molecule-1 (VCAM-1), and E-selectin in endothelial cells (ECs). These effectors encourage monocyte adhesion and infiltration into the intimal layer, followed by fatty streak formation that is attributed to an accumulation of lipid-laden macrophage foam cells.<sup>20,21</sup> Foam cell formation is characterized by the intracytoplasmic accumulation of cholesterol ester (CE), which is dependent on the balance between uptake of oxidized low-density lipoprotein (oxLDL) by CD36 and efflux of free cholesterol (FC) controlled by ATP-binding cassette transporter A1 (ABCA1).<sup>20,21</sup> To protect the cells against the toxicity of excessive FC accumulation, FC is esterified to CE by acyl-CoA:cholesterol acyltransferase-1 (ACAT-1). Other than the accumulation of macrophage foam cells, migration and proliferation of vascular smooth muscle cells (VSMCs), EC proliferation, and production of extracellular matrix (ECM) components, such as the collagens, matrix metalloproteinases (MMPs), fibronectin, and elastin, all contribute to progression of atherosclerotic plaques.<sup>21,22</sup>

In the present study, we assessed the modulatory effects of KP-10, *in vitro*, on the inflammatory response, proliferation, and adhesion (to monocytes) for HUVECs, foam cell formation in human monocyte-derived macrophages (HMDMs), and the migration, proliferation, and ECM production in human aortic smooth muscle cells (HASMCs). *In vivo* studies focused on the atherogenic effect of KP-10 and atheroprotective effect of a GPR54 antagonist in apolipoprotein E-deficient (ApoE<sup>-/-</sup>) mice.

## Methods

### Human Monocyte Primary Culture

Ethical approval was from the Tokyo University of Pharmacy and Life Sciences (Tokyo, Japan), with written informed consent obtained from all participants before blood draws. Human peripheral mononuclear cells were isolated from the blood of 20 healthy volunteers (8 male, 12 female; aged 19–25). Monocytes were purified using anti-CD14 antibody-conjugated magnetic microbeads (Miltenyi Biotec, Cambridge, MA). Primary monocytes were subsequently seeded into 3.5-cm dishes ( $1 \times 10^6$  cells/1 mL/dish)<sup>19–23</sup> and incubated at 37°C in a 5% CO<sub>2</sub> humidified incubator for 7 days in RPMI-1640 medium containing 10% human serum and the indicated concentrations of human KP-10 (Abgent, San Diego, CA). Media were changed every 3 days.

### Cholesterol Esterification Assay

HMDMs were differentiated by a 7-day culture with human serum and the indicated concentrations of KP-10, with a further incubation for 19 hours at 37°C/5% CO<sub>2</sub> with the same concentrations of KP-10, along with 50  $\mu$ g/mL of human oxLDL in the presence of 100  $\mu$ mol/L of [<sup>3</sup>H]oleate (PerkinElmer, Waltham, MA) conjugated with BSA.<sup>19–23</sup> Cellular lipids were extracted and the radioactivity attributed to cholesterol-[<sup>3</sup>H]oleate determined by thin-layer chromatography.

### Reverse-Transcription Polymerase Chain Reaction

HUVECs (Lonza, Basel, Switzerland) were incubated at 37°C in 5% CO<sub>2</sub> for 4 hours with an indicated concentration of KP-10 in EGM-2 (Lonza) containing 5% FBS. The mRNAs for TNF- $\alpha$ , IL-6, MCP-1, ICAM-1, VCAM-1, E-selectin, and glyceraldehyde-3-dehydrogenase were detected as described previously.<sup>21–23</sup>

### Monocyte Adhesion Assay

Confluent HUVECs cultured in 24-well plates were incubated at 37°C in a 5% CO<sub>2</sub> gassed incubator for 16 hours with EGM-2 containing 0.5% FBS for 16 hours and then treated with the indicated concentrations of KP-10 for 4 hours. Subsequently, human primary monocytes or THP-1 cells (Health Science Research Resources Bank, Osaka, Japan) were labeled with Cell trace calcein red-orange (Life Technologies, Carlsbad, CA) with  $1 \times 10^5$  cells added to each well of a HUVEC-seeded 24-well plate. After 1 hour, cells were washed 4 times, with human primary monocytes or THP-1 cells bound to HUVECs, and then examined by fluorescence microscopy (IX70; Olympus, Tokyo, Japan). Their adhesion was assessed using image analysis software (ImageJ; National Institutes of Health, Bethesda, MD).

## Proliferation Assay

HUVECs, HUVEC-derived EA.hy926 cells, or HASMCs at passage 2 to 8 were seeded into 96-well plates ( $1 \times 10^4$  cells/100  $\mu$ L/well) and incubated for 24 hours in DMEM or SmGM-2 containing 10% or 5% FBS, respectively. Cells were then incubated for a further 48 hours with the indicated concentrations of KP-10 in fresh media. Ten microliters of WST-8 solution (Cell Count Reagent SF; Nacalai Tesque, Inc, Kyoto, Japan) were then added to each well. After 1 hour of incubation, the quantity of formazan product was determined by reading absorbance at 450 nm using a Sunrise Remote R-micro plate reader (Tecan, Männedorf, Switzerland).<sup>19–23</sup>

## Migration Assay

HASMCs (Lonza) at passage 6 to 8 were seeded into 8-well culture slides ( $3 \times 10^3$  cells/250  $\mu$ L/well). Cells were incubated at 37°C in 5% CO<sub>2</sub> for 3 to 5 hours in SmGM-2 (Lonza) containing 5% FBS. HASMCs were then incubated for 15 hours with the indicated concentrations of angiotensin II (AngII) and/or KP-10 in serum-free SmGM. Cells were photographed at 10-minute intervals. The average migration distance of 10 cells randomly selected in each dish was measured using a BIOREVO BZ-9000 microscope (Keyence Corp, Osaka, Japan).<sup>19–23</sup>

## Apoptosis Assay

HASMCs or HUVEC-derived EA.hy926 cells were seeded into 12-well plates ( $3 \times 10^5$  cells/1 mL/well) and incubated at 37°C in a 5% CO<sub>2</sub> gassed incubator for 24 hours in the same conditioning media, followed by a 48-hour incubation with the indicated concentrations of KP-10. Cells were fixed with 4% paraformaldehyde. Terminal deoxynucleotidyl transferase-mediated deoxyuridine triphosphate-biotin nick end labeling (TUNEL) staining was then performed using an In Situ Apoptosis Detection Kit (Takara Bio, Shiga, Japan) as described previously.<sup>22</sup>

## Western Blotting

Aliquots of protein extracts (20  $\mu$ g) derived from HMDMs, HASMCs, HUVECs, and EA.hy926 cells were separated by 10% SDS-PAGE and then immunoblotted with antibodies raised against the following proteins: KP-10; GPR54 (LifeSpan BioSciences, Seattle, WA); phosphorylated protein kinase B (p-Akt); phosphorylated extracellular signal-regulated kinase 1 and 2 (ERK1/2); phosphorylated p38 (Cell Signaling Technology, Danvers, MA); cleaved caspase-3 (R&D Systems, Inc, Minneapolis, MN); and Bcl-2-associated X protein (Bax; Abcam, Cambridge, MA). Other antibodies used were same as described previously.<sup>19–23</sup>

## PAGE Zymography

The activities of MMP-2 and MMP-9 in culture supernatants of HASMCs were determined using a gelatin-zymography kit (Cosmo Bio USA, Inc, Carlsbad, CA) as described previously.<sup>21,22</sup>

## Animal Experiments

Protocols of 3 animal experiments were approved by the Institutional Animal Care and Use Committee of Tokyo University of Pharmacy and Life Sciences. A total of 66 of male spontaneously hyperlipidemic ApoE<sup>-/-</sup> mice in 2 strains, C57/B6 (KOR/StmSlc-ApoE<sup>shl</sup> mice) and BALB/c (KOR/StmSlc-ApoE<sup>shl</sup> mice), were purchased from Japan SLC (Hamamatsu, Japan). Mice were fed a high-cholesterol diet containing 16.5% fat, 1.25% cholesterol, and 0.5% sodium cholate (F2HFD1; Oriental Yeast, Tokyo, Japan), starting at 13 weeks of age.<sup>19–22</sup> Mice at 13 weeks of age were infused for 4 weeks with KP-10 and/or P234, a GPR54 antagonist (Peptide Institute, Osaka, Japan), using osmotic minipumps (Model 1002; Alzet; DURECT Corporation, Cupertino, CA). The time course and dose of KP-10 and P234 infusion were decided on the basis of others' previous and our preliminary data.<sup>13,24,25</sup>

Experiment 1 was performed to evaluate the dose-dependent effects of KP-10 on atherogenesis in 17 ApoE<sup>-/-</sup> mice (C57BL/6). At 13 weeks of age, 3 mice were euthanized as preinfusion controls. The remaining 14 were divided into 3 groups of 5, 4, and 5 and then infused with saline (vehicle) or KP-10 at doses of 5 and 12.5  $\mu$ g/kg per hour, respectively.

Experiment 2 was performed to evaluate the suppressive effects of P234 on KP-10-induced atherogenesis in 38 ApoE<sup>-/-</sup> mice (BALB/c). At 13 weeks of age, 7 mice were euthanized as a control before infusion. The remaining 31 were divided into 3 groups of 10, 10, and 11 and were then infused with saline, KP-10 (12.5  $\mu$ g/kg per hour) or KP-10 (12.5  $\mu$ g/kg per hour)+P234 (50  $\mu$ g/kg per hour), respectively.

Experiment 3 was performed to evaluate the preventive effects of P234 on endogenous KP-10-induced atherogenesis (the natural course of atherogenesis) in 10 ApoE<sup>-/-</sup> mice (BALB/c). From 13 to 17 weeks of age, 5 and 5 mice were infused with saline and P234 (50  $\mu$ g/kg per hour), respectively.

## Animal Measurements

Four weeks after commencing infusions into ApoE<sup>-/-</sup> mice, systolic and diastolic blood pressure (BP) was measured using the indirect tail-cuff method (Kent Scientific, Torrington, CT). Blood samples were collected after a 4-hour fast. Plasma concentrations of glucose and total cholesterol were

measured by enzymatic methods (Denka Seiken, Tokyo, Japan).<sup>19–22</sup> Plasma KP-10 concentration was measured by ELISA (Phoenix Pharmaceuticals Inc, Burlingame, CA) after extraction with a Sep-Pak C18 cartridge (Waters Associates, Milford, MA), as described before.<sup>24</sup>

### Atherosclerotic Lesion Assessment

Before and 4 weeks after the start of infusions, ApoE<sup>−/−</sup> mice were euthanized by exsanguination (total blood collection) under deep diethyl ether anesthesia. The whole aorta was washed by perfusion with PBS and fixed with 3.7% formaldehyde. The aorta was then excised from the aortic root to the abdominal area. The entire aorta and cross-sections of the aortic root were stained with Oil Red O for assessment of atherosclerotic lesions.<sup>19–22</sup> In aortic root, vascular inflammation, monocyte/macrophage infiltration, and VSMC contents were visualized by staining with antibodies for pentraxin-3 (Bioss, Woburn, MA), MOMA-2 (Millipore, Billerica, MA), or  $\alpha$ -smooth muscle actin ( $\alpha$ -SMA; Sigma-Aldrich, St. Louis, MO), respectively.<sup>19–22</sup> The positive stained areas were traced by an investigator blind to the treatment and measured using image analysis software (Adobe Photoshop and NIH ImageJ). The occupied areas of atheromatous plaque, vascular inflammation, and macrophage and VSMC contents were expressed as a percentage relative to the entire cross-section of the aortic wall. In addition, the ratios of macrophage content ( $\mu\text{m}^2$ )/VSMCs content ( $\mu\text{m}^2$ ) within the atheromatous plaques were calculated to evaluate the plaque stability.

### Statistical Analysis

Normality was tested with the Kolmogorov–Smirnov test. Normally distributed data are presented as mean $\pm$ SEM and non-normally distributed data as median [25%, 75%]. Differences between 2 groups were assessed by an unpaired Student *t* test. The nonparametric Mann–Whitney *U* test was used if data were not normally distributed. Multiple comparisons were made among  $\geq 3$  groups using 1-way ANOVA followed by the Bonferroni post-hoc test. Statistical analyses were performed using Statview-J 5.0 (SAS Institute Inc, Cary, NC). A value of  $P < 0.05$  was considered significant.

## Results

### Expression of GPR54 in Human Vascular Cells

First, the expression of KP-10 receptor (GPR54) was investigated in human vascular cells used in this study. GPR54 was expressed at high levels in human monocytes, HMDMs, HASMCs, HUVECs, and EA.hy926 cells (Figure 1A).

### Effects of KP-10 on Human Monocyte Adhesion to HUVECs

KP-10 significantly increased adhesion of THP-1 cells to HUVECs by  $\approx 10$ -fold at 10  $\mu\text{mol/L}$  (Figure 1B). Pretreatment with the GPR54 antagonist, P234 (20  $\mu\text{mol/L}$ ), significantly inhibited KP-10 (10  $\mu\text{mol/L}$ )-induced adhesion of THP-1 cells to HUVECs (Figure 1C). These results indicated that KP-10 increases the adhesion of THP-1 cells to HUVECs by GPR54.

In a similar degree to the above result, the adhesion of human primary monocytes to HUVECs was also significantly increased by KP-10 (Figure 1D).

### Effects of KP-10 on Inflammatory Response, Proliferation, and Apoptosis in Human ECs

KP-10 markedly enhanced mRNA expression for TNF- $\alpha$ , IL-6, MCP-1, ICAM-1, VCAM-1, and E-selectin in HUVECs (Figure 2A). KP-10 significantly increased the protein expression of ICAM-1 and VCAM-1 in HUVECs (Figure 2B) in parallel with the increases in mRNA levels (Figure 2A).

KP-10 significantly suppressed the proliferation of EA.hy926 cells, but not HUVECs, in a concentration-dependent manner, with a maximal reduction by 28% at 10  $\mu\text{mol/L}$  (Figure 2C). In addition, the induction of apoptosis was not evident at 10  $\mu\text{mol/L}$  of KP-10 in EA.hy926 cells (Figure 2D).

### Effects of KP-10 on Foam Cell Formation and Related Protein Expression in HMDMs

KP-10 significantly enhanced oxLDL-induced foam cell formation by 21% at 5  $\mu\text{mol/L}$  in HMDMs (Figure 2E). KP-10 also significantly increased protein expression of CD36 and ACAT-1 and did not show a significant change in ABCA1 expression in HMDMs (Figure 2F).

### Effects of KP-10 on Migration, Proliferation, and Apoptosis in HASMCs

KP-10 itself had no significant effect on the migration of HASMCs (Figure 3A). AngII significantly increased the migration of HASMCs (Figure 3A). However, KP-10 significantly suppressed the AngII-stimulated migration of HASMCs (Figure 3A). KP-10 also significantly suppressed the proliferation of HASMCs in a concentration-dependent manner, with a maximal reduction by 14% at 10  $\mu\text{mol/L}$  (Figure 3B). Moreover, KP-10 (10  $\mu\text{mol/L}$ ) significantly induced apoptosis of HASMCs (Figure 3C).

KP-10 significantly suppressed the proliferative phenotype (SMemb) and Akt protein phosphorylation in HASMCs. In contrast, KP-10 significantly increased the protein

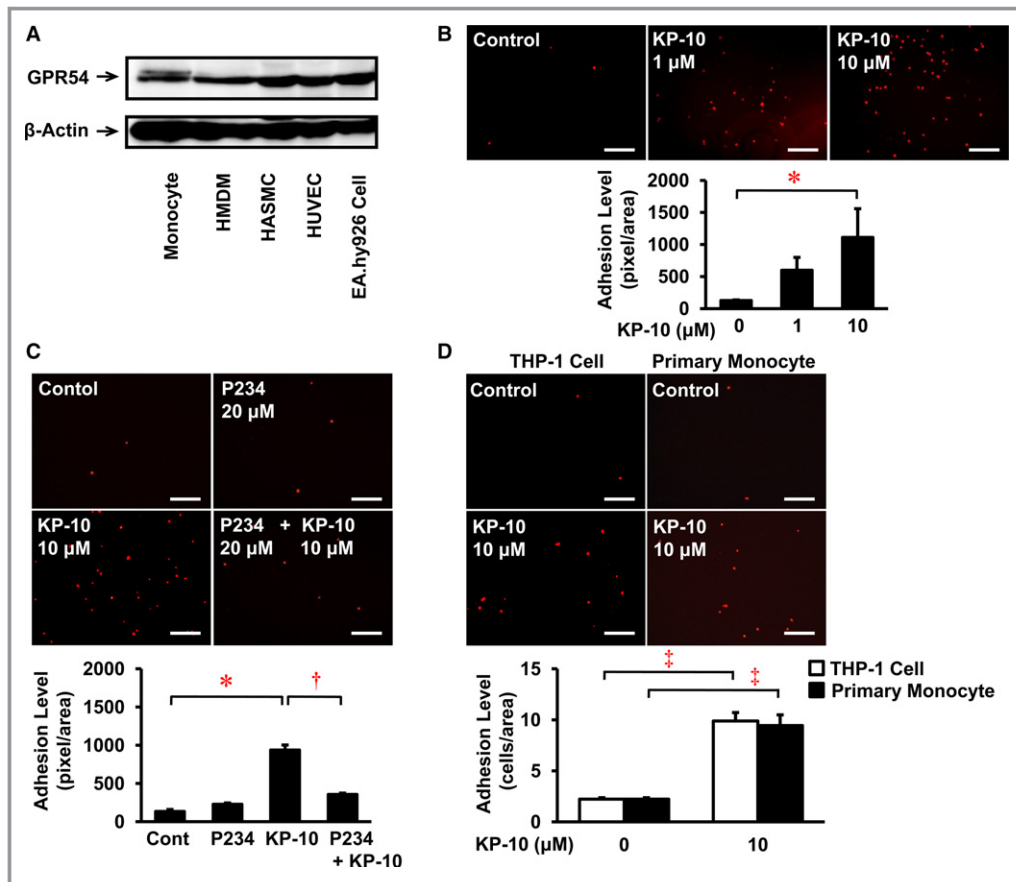


**Figure 1.** Expression of GPR54 in human vascular cells and effects of KP-10 on monocyte-HUVEC adhesion. A, Aliquots of protein extracts (30 μg) derived from human monocytes, HMDMs, HASMCs, HUVECs, and EA.hy926 cells were separated by 10% SDS-PAGE and then immunoblotted with anti-GPR54 antibody. β-actin served as a loading control. Representative images are shown from 4 independent experiments. B, HUVECs were incubated with the indicated concentrations of KP-10 for 4 hours, followed by a 1-hour incubation with calcein red-orange-labeled THP-1 cells. C, HUVECs were pretreated with or without the GPR54 antagonist, P234, for 30 minutes and incubated with KP-10 for 4 hours, followed by 1-hour incubation with labeled THP-1 cells. D, HUVECs were incubated with KP-10 for 4 hours, followed by a 1-hour incubation with labeled THP-1 cells or labeled human primary monocytes. Cell adhesion was determined by fluorescence microscopy. Scale bar=100 μm. All experiments were independently performed 3 times (each n=3; in B, C, and D). \**P*<0.05, †*P*<0.05, ‡*P*<0.0005. HASMC indicates human aortic smooth muscle cell; HMDM, human monocyte-derived macrophage; HUVEC human umbilical vein endothelial cell; KP-10, kisspeptin-10.

phosphorylation of ERK1/2 and p38 and also increased the protein expression of Bax and cleaved caspase-3 in HASMCs (Figure 3D).

### Effects of KP-10 on ECM Expression in HASMCs

KP-10 did not significantly alter the protein expression of collagen-1, collagen-3, fibronectin, and elastin in HASMCs (Figure 3E and Figure S1). However, KP-10 showed a tendency to increase the protein expression of MMP-2 and MMP-9 (Figure S1). Furthermore, zymography revealed that KP-10 significantly enhanced the activities of MMP-2 and MMP-9 (Figure 3F).

### Effects of KP-10 on Atherosclerotic Lesion Development in ApoE<sup>-/-</sup> Mice

We evaluated the effects of KP-10 and the GPR54 antagonist P234 on the development of atherosclerotic lesions in 2 different strains of ApoE<sup>-/-</sup> mice (C57/B6 and BALB/c). In ApoE<sup>-/-</sup> mice (C57/B6), the (entire) surface and cross-sectional area of the root (plaque size) of aortic atherosclerotic lesions with pentraxin-3-positive area, monocyte/macrophage infiltration, and VSMC content as well as plasma total cholesterol concentration were significantly increased at 17 weeks of age compared with 13 weeks of age (Figure 4A: a, b, e, f, i, j, m, n, q, r, 4B through 4F; Table 1). By 17 weeks

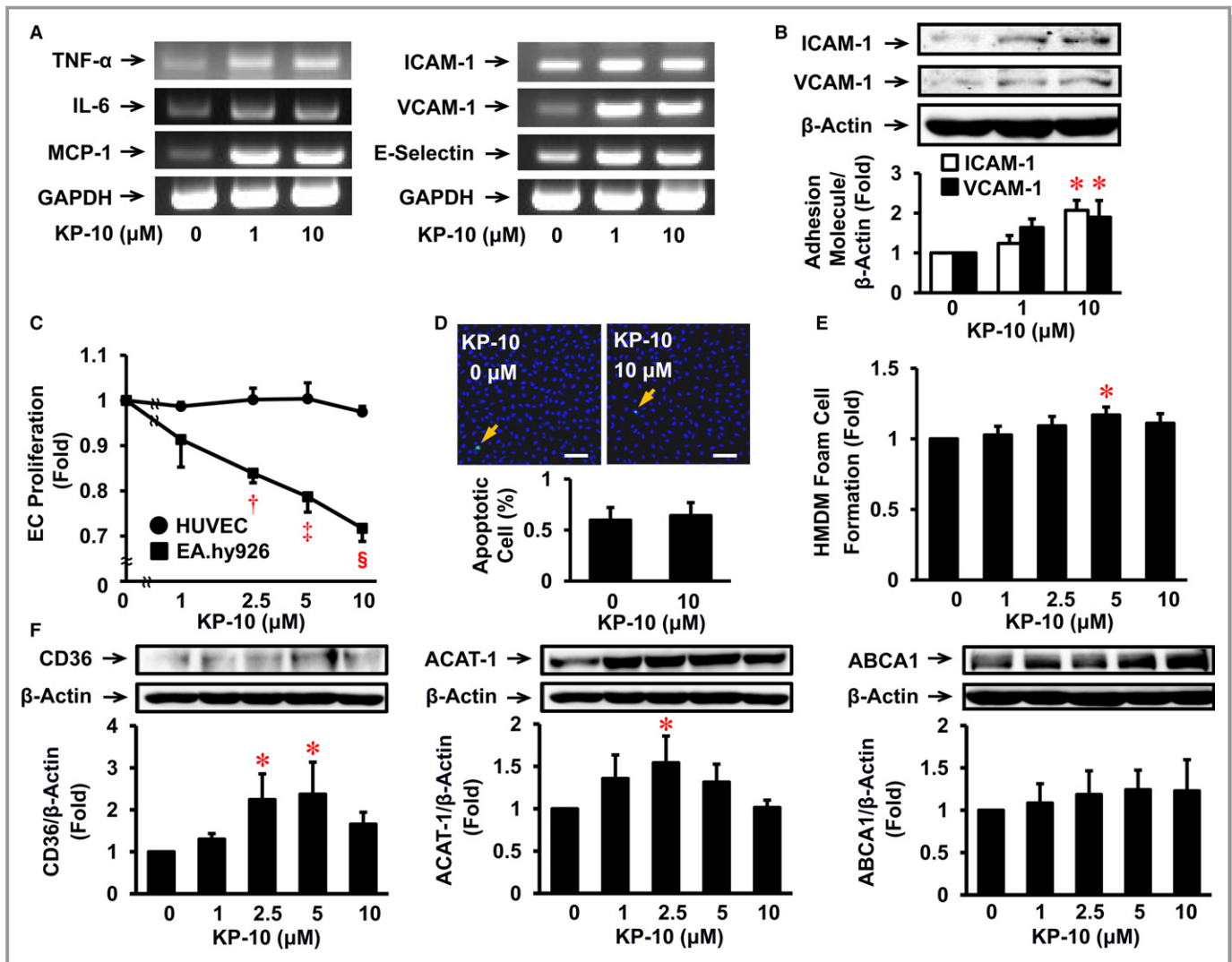


**Figure 2.** Effects of KP-10 in inflammatory response and proliferation in human ECs and foam cell formation in HMDMs. A, HUVECs were treated with the indicated concentrations of KP-10 for 2 hours. mRNA expressions of TNF- $\alpha$ , IL-6, MCP-1, ICAM-1, VCAM-1, and E-selectin were analyzed by reverse transcription-polymerase chain reaction. Representative images are shown from 3 independent experiments. B, HUVECs were incubated with indicated concentrations of KP-10 for 4 hours and harvested for immunoblot to evaluate ICAM-1 and VCAM-1 protein expression (n=3). Representative images are shown; the graph indicates densitometry data following normalization relative to  $\beta$ -actin. C, HUVECs or EA.hy926 cells were incubated with indicated concentrations of KP-10 for 48 hours. Proliferation was determined by WST-8 assay (n=4). D, EA.hy926 cells treated with KP-10 for 48 hours were stained to detect apoptotic cells (green) using the TUNEL method. DAPI was incorporated as a nuclear (blue). The graph indicates the percentage of apoptotic cells in 3 independent experiments. Scale bar=100  $\mu$ m. E, Human monocytes were incubated with the indicated concentrations of KP-10 for 7 days, followed by a 19-hour incubation with oxLDL and [ $^3$ H] oleate along with KP-10. Foam cell formation was determined from the intracellular radioactivity of cholesterol-[ $^3$ H]oleate (n=9). Baseline of control=8.0 $\pm$ 1.6 nmol/mg cell protein. F, Before the addition of oxLDL, HMDMs were harvested for immunoblot analyses using anti-CD36, ACAT-1, and ABCA1 (n=7). \* $P$ <0.05;  $^{\dagger}P$ <0.01;  $^{\ddagger}P$ <0.005;  $^{\S}P$ <0.0001 vs 0  $\mu$ mol/L of KP-10. ABCA1 indicates ATP-binding cassette transporter A1; ACAT-1, acyl-CoA:cholesterol acyltransferase-1; DAPI, 4',6-diamidino-2-phenylindole; EC, endothelial cell; HMDM, human monocyte-derived macrophage; HUVEC, human umbilical vein endothelial cell; ICAM-1, intercellular adhesion molecule-1; IL-6, interleukin-6; KP-10, kisspeptin-10; MCP-1, monocyte chemotactic protein-1; oxLDL, oxidized low-density lipoprotein; TNF- $\alpha$ , tumor necrosis factor- $\alpha$ ; TUNEL, terminal deoxynucleotidyl transferase-mediated deoxyuridine triphosphate-biotin nick end labeling; VCAM-1, vascular adhesion molecule-1.

of age, plasma KP-10 concentration was significantly elevated in mice infused with a high dose of KP-10 (12.5  $\mu$ g/kg per hour) compared with the vehicle control (Table 1). A high dose of KP-10 (12.5  $\mu$ g/kg per hour) significantly enhanced the aortic atherosclerotic lesion area and atheromatous plaque

size (Figure 4A: b, d, f, h, 4B and 4C), with significant increases in pentraxin-3-positive area and monocyte/macrophage infiltration and a significant decrease in VSMC content (Figure 4A: j, l, n, p, r, t, 4D through 4F). There were no significant differences in body weight, food intake, systolic

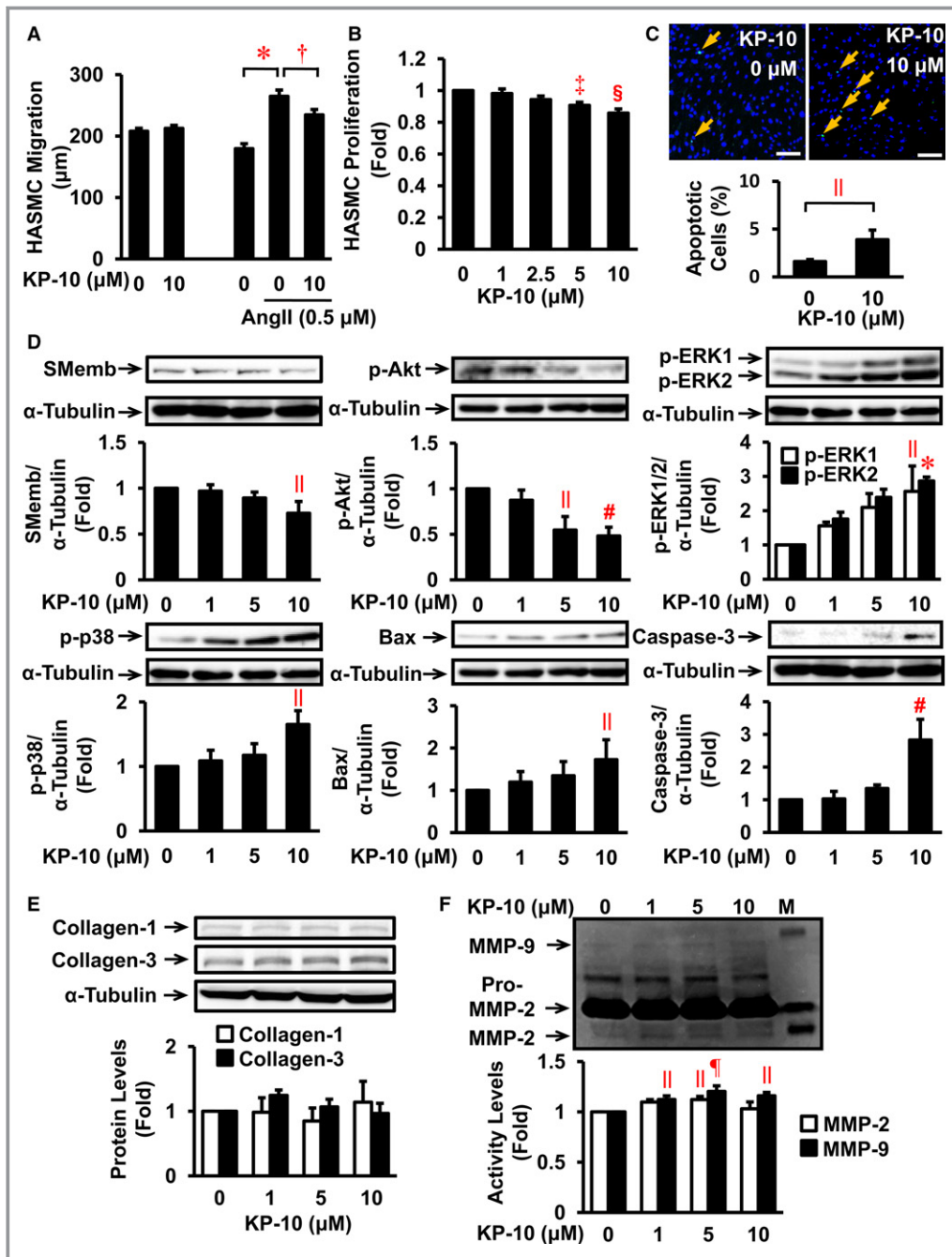


**Figure 3.** Effects of KP-10 on migration, proliferation, apoptosis, and ECM production in HASMCs. A, Migration of HASMCs treated with the indicated concentrations of KP-10 in the absence or presence of AngII was determined using a BIOREVO BZ-9000 microscope (n=3). \* $P < 0.0001$ ; † $P < 0.05$ . B, Proliferation of HASMCs was determined by WST-8 assay following a 48-hour incubation with the indicated concentrations of KP-10 (n=5). C, HASMCs treated with KP-10 for 48 hours were stained to detect apoptotic cells (green) using the TUNEL method. DAPI was incorporated as a nuclear (blue). The graph indicates the percentage of apoptotic cells in 3 independent experiments. Scale bar=100 µm. D and E, HASMCs were incubated with KP-10 for 24 hours and harvested for immunoblots of mitogenic phenotype and signaling, collagen-1, and collagen-3 (n=3–4). F, In the same experiments, MMP-2 and MMP-9 activities in culture supernatants were determined by gelatin zymography (n=4). ‡ $P < 0.001$ ; § $P < 0.0005$ ; || $P < 0.05$ ; # $P < 0.01$ ; ¶ $P < 0.005$  vs 0 µmol/L of KP-10. AngII indicates angiotensin II; Bax, Bcl-2-associated X protein; DAPI, 4',6-diamidino-2-phenylindole; ECM, extracellular matrix; ERK, extracellular signal-regulated kinase; HASMC, human aortic smooth muscle cell; KP-10, kisspeptin-10; MMP, matrix metalloproteinase; p-Akt, phosphorylated protein kinase B.

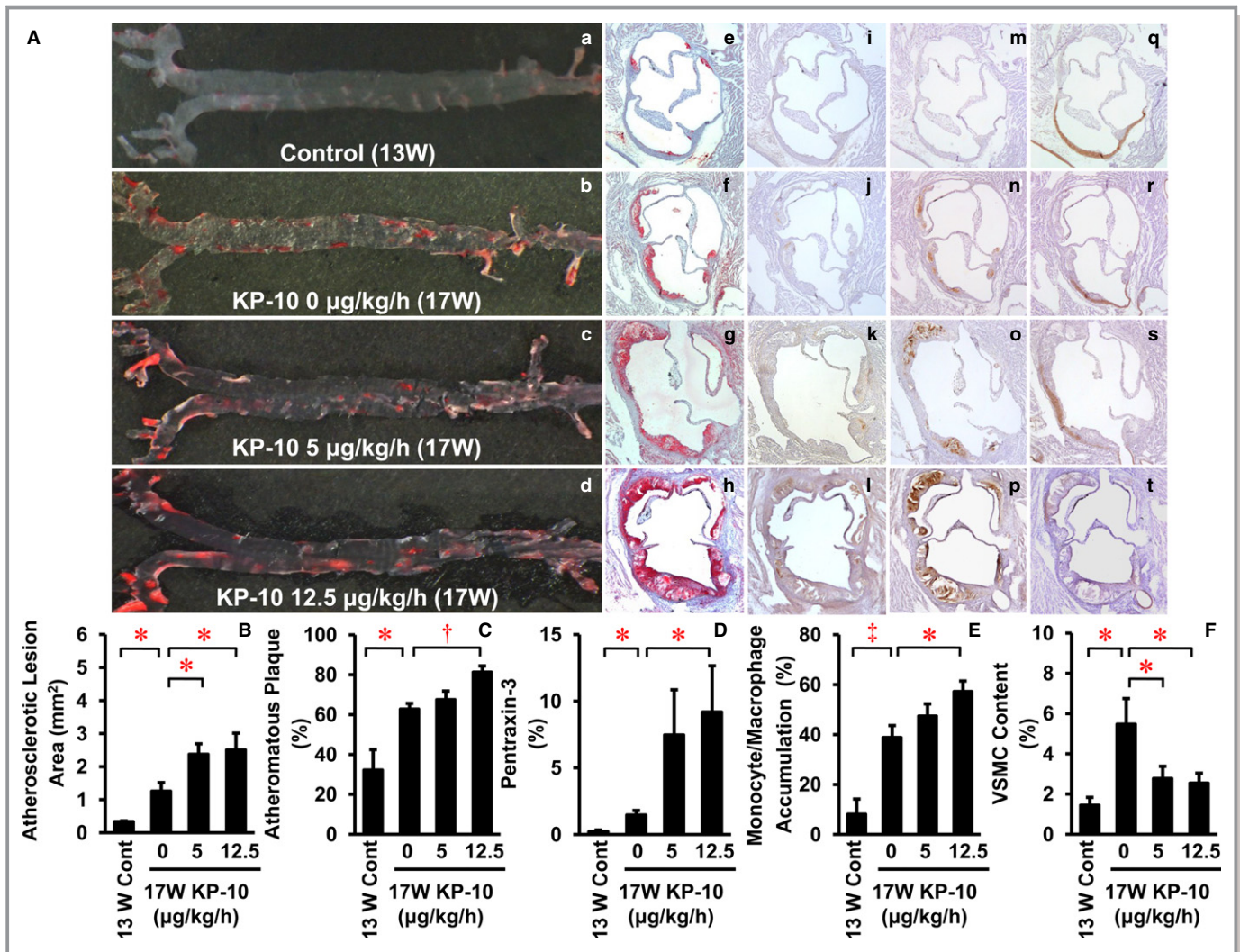


**Figure 4.** Dose-dependent effects of KP-10 on atherosclerotic lesion development in ApoE<sup>-/-</sup> mice (experiment 1). Of 17 ApoE<sup>-/-</sup> mice (C57/B6) at 13 weeks of age, 3 were euthanized before infusion and 5, 4, and 5 were infused with KP-10 at doses of 0, 5, 12.5 µg/kg per hour by osmotic minipumps for 4 weeks. The aortic surface was stained with Oil Red O (A: a through d). Cross-sections of the aortic root were stained with Oil Red O (A: e through h), with immunostains for pentraxin-3 (A: i through l), MOMA-2 (A: m through p), or α-SMA (A: q through t). Comparisons of atherosclerotic lesion area (B), atheromatous plaque (C), pentraxin-3 expression (D), monocyte/macrophage accumulation (E), and VSMC content (F) among the 4 groups. \*P<0.05; †P<0.005; ‡P<0.01. ApoE<sup>-/-</sup> indicates apolipoprotein E deficient; KP-10, kisspeptin-10; α-SMA, α-smooth muscle actin; VSMC, vascular smooth muscle cell.

and diastolic BP, and plasma concentrations of either total cholesterol or glucose among the 3 groups of ApoE<sup>-/-</sup> mice at 17 weeks of age (Table 1).

In ApoE<sup>-/-</sup> mice (BALB/c), aortic atherosclerotic lesion area and atheromatous plaque size with pentraxin-3-positive area and monocyte/macrophage and VSMC contents as well as plasma total cholesterol concentration were similarly increased at 17 weeks of age compared with 13 weeks of age (Figure 5A: a, b, e, f, i, j, m, n, q, r, 5B through 5F; Table 2). Infusion of KP-10 (12.5 µg/kg per hour) significantly enhanced aortic atherosclerotic lesion area and atheromatous plaque size (Figure 5A: b, c, f, g, 5B and 5C), with a significant increase in monocyte/macrophage

infiltration (with an increase tendency in pentraxin-3-positive area) and a significant decrease in VSMC content (Figure 5A: j, k, n, o, r, s, 5D through 5F). At 17 weeks of age, plasma KP-10 concentration was significantly elevated in ApoE<sup>-/-</sup> mice infused with KP-10 or KP-10+P234 compared to the vehicle control (Table 2). However, there were no significant differences in body weight, food intake, systolic and diastolic BP, and plasma concentrations of total cholesterol and glucose among the 3 groups of ApoE<sup>-/-</sup> mice at 17 weeks of age (Table 2). Compared with KP-10 infusion, coinfusion of KP-10+P234 significantly suppressed aortic atherosclerotic lesion area and atheromatous plaque size (Figure 5A: c, d, g, h, 5B and 5C), with a significant



**Table 1.** Characteristics and Laboratory Data of ApoE<sup>-/-</sup> Mice (Experiment 1)

Parameter	ApoE <sup>-/-</sup> Mice (C57/B6)			
	13W Control	17W Control 0 µg/kg per hour	17W KP-10 5 µg/kg per hour	17W KP-10 12.5 µg/kg per hour
N	3	5	4	5
Body weight, g	27.7±0.76	30.4±0.60*	29.8±0.85	29.2±0.58
Food intake, g/day	NE	5.9±0.4	6.4±0.4	6.3±0.4
Systolic BP, mm Hg	109.0±4.5	105.0±1.8	101.5±4.8	104.1±1.6
Diastolic BP, mm Hg	89.0±7.0	85.4±1.0	81.1±4.0	83.3±2.7
Total cholesterol, mg/dL	322.0±15.8	1705.5±116.9*	1714.9±148.5*	1776.6±53.2*
Glucose, mg/dL	246.2±73.3	353.4±37.0	231.3±38.1	312.4±44.1
KP-10, ng/mL	5.65±2.14	5.85±2.21	6.37±2.16	19.54±5.01 <sup>†</sup>

Mean±SEM. ApoE<sup>-/-</sup> indicates apolipoprotein E deficient; BP, blood pressure; KP-10, kisspeptin-10; NE, not examined.

\*P<0.05 vs 13W control.

<sup>†</sup>P<0.05 vs 17W control.

decrease in monocyte/macrophage infiltration (with a decrease tendency in pentraxin-3-positive area) and a significant increase in VSMC content (Figure 5A: k, l, o, p, s, t, 5D through 5F).

Last, the preventive effect of P234 alone on endogenous KP-10-induced atherogenesis was determined in ApoE<sup>-/-</sup> mice (BALB/c). P234 infusion significantly prevented both aortic atherosclerotic lesion area and atheromatous plaque size (Figure 6A: b, c, e, f, 6B and 6C), without significant changes in pentraxin-3-positive area, monocyte/macrophage infiltration, and VSMC content. There were no significant differences in body weight, food intake, systolic and diastolic BP, and plasma concentrations of total cholesterol and glucose between the 2 groups of ApoE<sup>-/-</sup> mice at 17 weeks of age (Table 3).

### Effects of KP-10 and P234 on Atheromatous Plaque Instability in ApoE<sup>-/-</sup> Mice

In experiment 2, we calculated the ratio of macrophage content/VSMC content within atheromatous plaques as an index of plaque instability in ApoE<sup>-/-</sup> mice. The ratio tended to increase with age (13–17 weeks of age) and was significantly increased by KP-10 and reversed to the control level by P234 (Figure 7). This finding suggests that KP-10 may induce plaque instability and P234 may contribute to stabilize atheromatous plaque.

### Discussion

We now provide the first evidence to show that KP-10 stimulates the inflammatory response in HUVECs, monocyte adhesion to HUVECs, and macrophage foam cell formation in vitro and accelerates the development of atherosclerotic

lesions with increased monocyte/macrophage infiltration and pentraxin-3 expression in ApoE<sup>-/-</sup> mice in vivo. In addition, KP-10 suppresses the migration and proliferation and enhances apoptosis and MMPs activity in HASMCs, suggesting that KP-10 may induce plaque instability. Although each change with KP-10 in a variety of cellular and molecular phenomena in vitro seems to be weak, united, all exert a greatly and visibly stimulatory effect of KP-10 on atherogenesis in vivo. In the present study, we also show that the GPR54 antagonist significantly cancelled the exogenous KP-10-stimulated atheromatous plaque development and instability in ApoE<sup>-/-</sup> mice. In high-cholesterol-diet-fed ApoE<sup>-/-</sup> mice from 13 to 17 weeks of age, the development of aortic atherosclerotic lesions is more closely linked to the marked increase in plasma total cholesterol levels compared with a little increase in plasma endogenous KP-10 levels (+200 pg/mL; Tables 1 and 2). Nevertheless, the GPR54 antagonist was able to prevent significantly the development of atherosclerotic lesions in ApoE<sup>-/-</sup> mice.

Both KPs and GPR54 are expressed in ECs, macrophages, cardiomyocytes, pancreas, hypothalamus, and extravillous trophoblast.<sup>8,11,12,26</sup> In our preliminary investigation (Data S1), both KP-10 and GPR54 are expressed at high levels in human coronary atherosclerotic lesions (Figure S2A). In the present study, GPR54 is expressed in human ECs, monocytes, macrophages, and VSMCs. Ovarian *kiss1* and *kiss1r* expressions are increased in aged mice compared to reproductive-age mice.<sup>27</sup> Loss of function of GPR54 or KPs induces hypogonadotropic hypogonadism.<sup>26,28,29</sup> Bowe et al have shown that KPs stimulate the release of insulin from the pancreas.<sup>30</sup> Actually, *kiss1r*-knockout mice exhibit the phenotypes of glucose intolerance and obesity.<sup>31</sup> KPs also regulate vascular tone as a constrictor.<sup>32</sup> However, in our

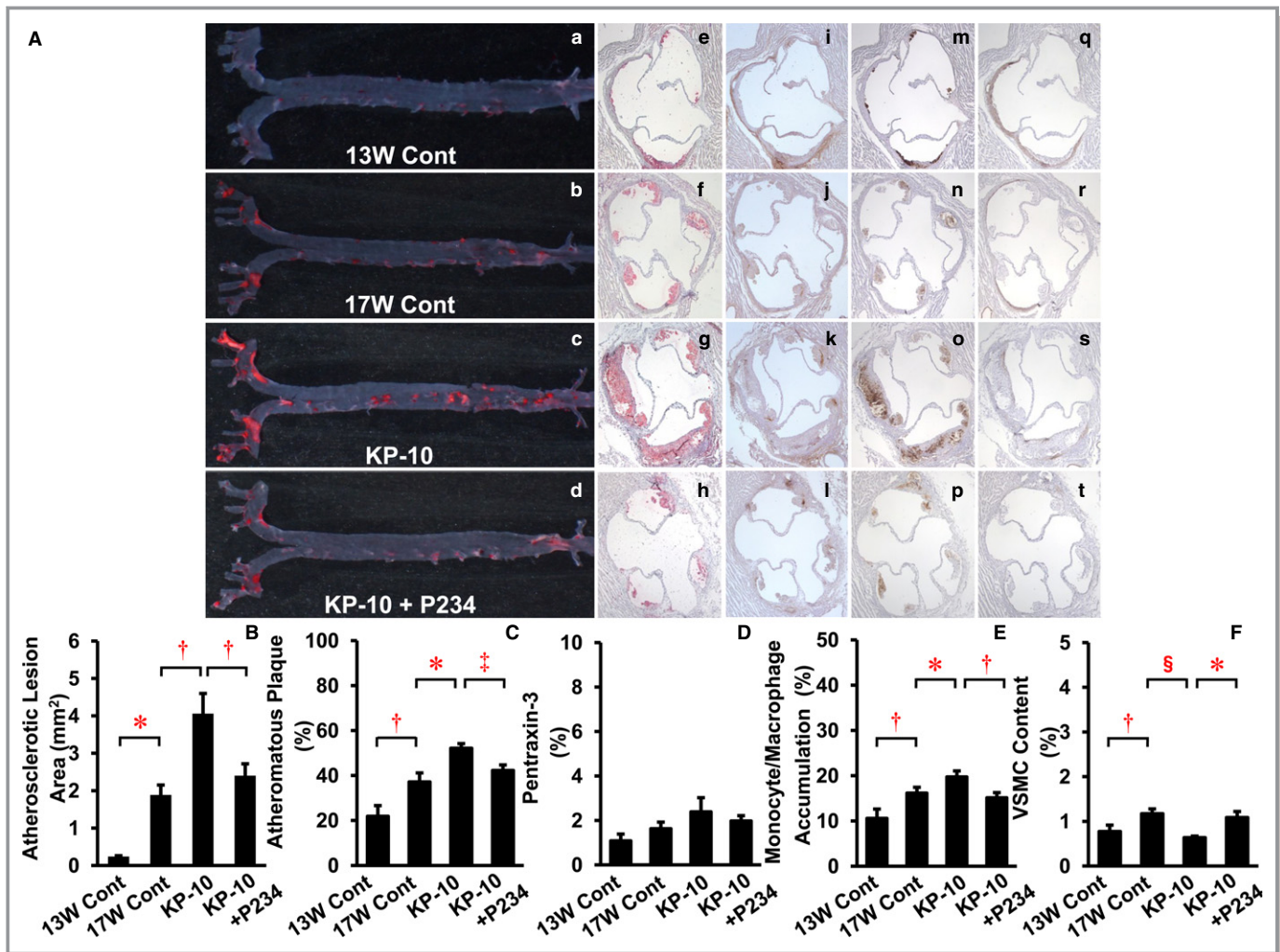


**Figure 5.** Suppressive effects of P234 (GPR54 antagonist) on KP-10-induced atherosclerotic lesion development in ApoE<sup>-/-</sup> mice (experiment 2). Of 38 ApoE<sup>-/-</sup> mice (BALB/c) at 13 weeks of age, 7 were euthanized before infusion and 10, 10, and 11 were infused with KP-10 (0 μg/kg per hour), KP-10 (12.5 μg/kg per hour), and KP-10 (12.5 μg/kg per hour)+P234 (50 μg/kg per hour) by osmotic minipumps for 4 weeks. The aortic surface was stained with Oil Red O (A: a through d). Cross-sections of the aortic root were stained with Oil Red O (A: e through h), with immunostains for pentraxin-3 (A: i through l), MOMA-2 (A: m through p), or α-SMA (A: q through t). Comparisons of atherosclerotic lesion area (B), atheromatous plaque (C), pentraxin-3 expression (D), monocyte/macrophage accumulation (E), and VSMC content (F) among the 4 groups. \*P<0.005; †P<0.05; ‡P<0.001; §P<0.0005. ApoE<sup>-/-</sup> indicates apolipoprotein E deficient; KP-10, kisspeptin-10; α-SMA, α-smooth muscle actin; VSMC, vascular smooth muscle cell.

study, chronic infusion of KP-10 did not affect body weight, plasma glucose level, and BP in ApoE<sup>-/-</sup> mice.

Pentraxin-3 is well known to reflect vascular inflammation derived from mainly ECs followed by VSMCs and macrophages and also is associated with apoptosis and plaque vulnerability.<sup>33-36</sup> In the present study, increased pentraxin-3 expression and increased activities of MMP-2 and MMP-9 as well as apoptosis induction in VSMCs by KP-10 may be associated with atherosclerotic plaque instability. Previous reports showed that KPs downregulated MMP-2 and MMP-9 at both the transcriptional and protein levels in human renal carcinoma KU19-20 cells and fibrosarcoma HT-1080 cells, respectively.<sup>37,38</sup>

However, our study showed that KP-10 promoted MMP-2 and MMP-9 activities in HASMCs. The discrepancy may be attributed to differences in cell types and the methods of KP-10 addition into these cells. Further studies are needed to elucidate whether knockout of KP-10 in ApoE<sup>-/-</sup> mice may suppress the progression and rupture of atherosclerotic plaques.

Different cell types in vitro and different animal backgrounds in vivo were used in the present study. First, EA.hy926 is a hybrid cell line derived by fusion of HUVEC with A549 cells. Compared with HUVECs, EA.hy926 cells were more convenient for our WST-8 assay to determine cell proliferation without inducing apoptosis.<sup>39</sup> In contrast,

**Table 2.** Characteristics and Laboratory Data of ApoE<sup>-/-</sup> Mice (Experiment 2)

Parameter	ApoE <sup>-/-</sup> Mice (BALB/c)			
	13W Control	17W Control 0 µg/kg per hour	17W KP-10 12.5 µg/kg per hour	17W KP-10+P234
N	7	10	10	11
Body weight, g	26.7±1.2	28.0±0.8	29.2±1.2	28.3±0.7
Food intake, g/day	NE	5.0±0.6	5.4±0.3	5.2±0.5
Systolic BP, mm Hg	93.4±1.0	92.8±1.3	94.2±1.2	93.3±1.6
Diastolic BP, mm Hg	72.6±1.0	71.8±1.4	74.3±1.0	73.7±1.5
Total cholesterol, mg/dL	575.0±82.4	2140.3±52.0*	2028.6±42.7*	1930.0±112.4*
Glucose, mg/dL	199.3±35.4	279.8±21.5	265.0±20.2	282.6±28.0
KP-10, ng/mL	0.4±0.1	0.6±0.1	1.6±0.2 <sup>†</sup>	2.4±0.4 <sup>‡</sup>

Mean±SEM. ApoE<sup>-/-</sup> indicates apolipoprotein E deficient; BP, blood pressure; KP-10, kisspeptin-10; NE, not examined.

\*P<0.05 vs 13W control.

<sup>†</sup>P<0.005; <sup>‡</sup>P<0.0001 vs 17W control.

HUVECs were more adequate to analyze the changes in inflammatory molecules' expression with KP-10, because HUVECs may involve the abundant of cyclooxygenase 2.<sup>40</sup>

According to the above reasons, we have used these cell lines in our previous studies.<sup>21,22</sup> The present study revealed that KP-10 significantly decreased the proliferation of EA.hy926

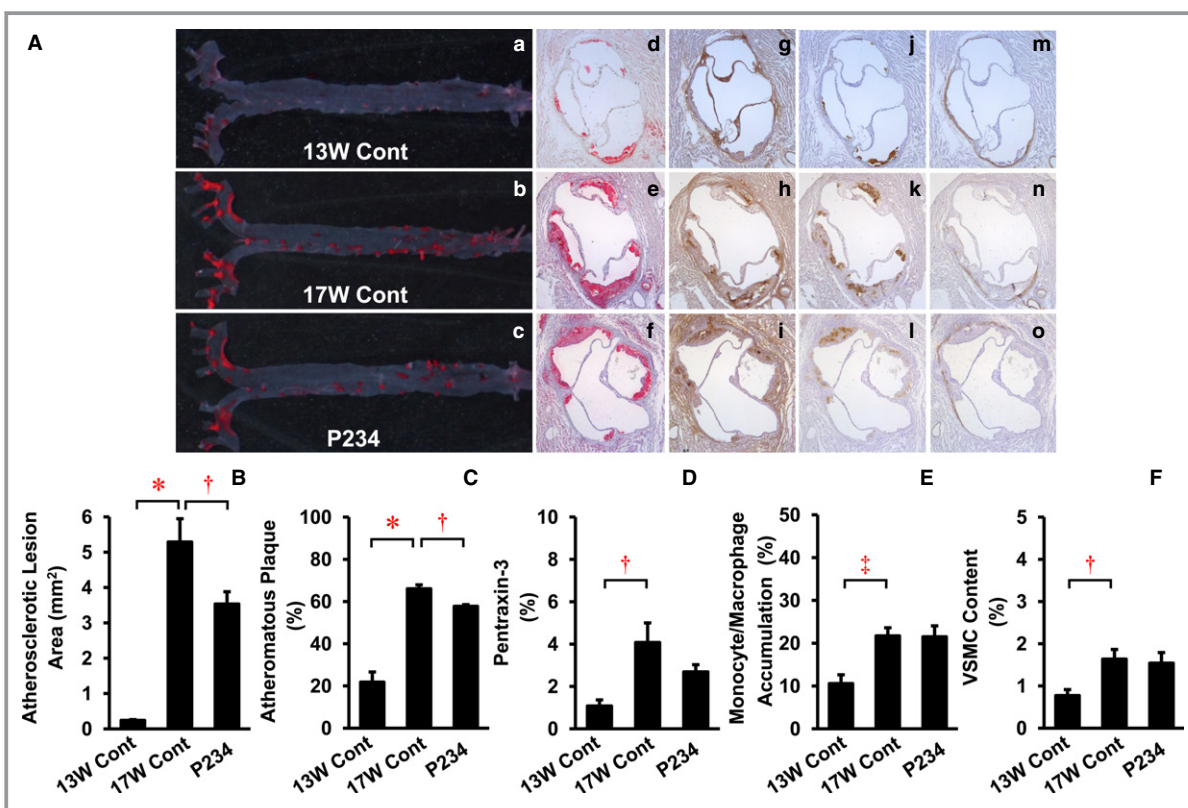


**Figure 6.** Preventive effects of P234 (GPR54 antagonist) on endogenous KP-10-induced atherosclerotic lesion development in ApoE<sup>-/-</sup> mice (experiment 3). Of 17 ApoE<sup>-/-</sup> mice (BALB/c) at 13 weeks of age, 7 were euthanized before infusion and 5 and 5 were infused with saline and P234 (50 µg/kg per hour) by osmotic minipumps for 4 weeks. The aortic surface was stained with Oil Red O (A: a through c). Cross-sections of the aortic root were stained with Oil Red O (A: d through f), with immunostains for pentraxin-3 (A: g through i), MOMA-2 (A: j through l), or α-SMA (A: m through o). Comparisons of atherosclerotic lesion area (B), atheromatous plaque (C), pentraxin-3 expression (D), monocyte/macrophage accumulation (E), and VSMC content (F) among the 3 groups. \*P<0.0001, <sup>†</sup>P<0.05, <sup>‡</sup>P<0.01. ApoE<sup>-/-</sup> indicates apolipoprotein E deficient; KP-10, kisspeptin-10; α-SMA, α-smooth muscle actin; VSMC, vascular smooth muscle cell.

**Table 3.** Characteristics and Laboratory Data of ApoE<sup>-/-</sup> Mice (Experiment 3)

Parameter	ApoE <sup>-/-</sup> Mice (BALB/c)		
	13W Control	17W Control 0 µg/kg per hour	17W P234 50 µg/kg per hour
N	7	5	5
Body weight, g	26.7±1.2	27.1±0.5	28.2±0.4
Food intake, g/day	NE	4.3±0.1	4.5±0.2
Systolic BP, mm Hg	93.4±1.0	96.1±0.7	97.0±0.7
Diastolic BP, mm Hg	72.6±1.0	75.8±1.1	75.2±0.8
Total cholesterol, mg/dL	575.0±82.4	2660.2±89.8*	2534.1±167.5*
Glucose, mg/dL	199.3±35.4	241.7±26.4	289.0±42.4

Mean±SEM. ApoE<sup>-/-</sup> indicates apolipoprotein E deficient; BP, blood pressure; NE, not examined.

\*P<0.0001 vs 13W control.

cells, but not HUVECs. Second, because of the stopping of supplying from a commercial mouse breeder, we unavoidably used 2 strains of ApoE<sup>-/-</sup> mice. However, we set control mice before and after infusion with saline in each experiment. Therefore, they are reliable data in the independent protocol of experiments.

The signal transduction pathways for KP-10 have yet to be identified. Our study suggests that KP-10 suppresses the

migration and proliferation, and induces apoptosis and MMPs production associated with the downregulation of Akt phosphorylation and the upregulation of ERK1/2 and p38 phosphorylation and caspase-3 expression in VSMCs. Kotani et al<sup>3</sup> showed that the suppressive effects of KPs on proliferation in Chinese hamster ovary cells expressing human or rat GPR54, with phosphorylation of ERK1/2 and p38. In our study, it is reasonable that KP-10 suppresses proliferation of EA.hy926 cells and HASMCs by phosphorylation of ERK1/2 and p38.

The physiological relevance of the KP-10 concentrations used in our in vitro and in vivo experiments warrants further discussion. First, the concentrations of KP-10 needed to influence multiple HUVEC, HMDM, and HASMC responses were considerably high (maximum ≈7400-fold) compared with average plasma concentration of KP-10 (1.35 nmol/L [1.05 ng/mL]) in 28 healthy volunteers (Figure S2B). In the vascular wall, ECs and macrophages generate large amounts of KP-10 in an autocrine/paracrine manner. Plasma KP-54 concentration increases by 1000- to 10 000-fold during pregnancy.<sup>41</sup> Consequently, it is not surprising that local levels of KP-10 were increased in a similar degree. Second, the concentration of KP-10 in serum obtained from a healthy human volunteer was 0.32 nmol/L (0.41 ng/mL) in our study. Therefore, the 10% concentration added to culture medium for HMDMs (32 pmol/L) was negligible compared with the concentrations of KP-10 added. Third, the concentrations of KP-10 differed in terms of the inflammation responses that they provoked in HUVECs, as well as their influence on monocyte-HUVEC adhesion, macrophage foam cell formation and effector expression, HASMC migration and proliferation, and ECM production. This likely reflects the different cell types used and their intracellular signals. Fourth, the dose of KP-10 (12.5 µg/kg per hour) infusion into mice is 9.6-fold higher compared with its dose (1.3 µg/kg per hour [1.0 nmol/kg per hour]) used in humans.<sup>42</sup> It is generally accepted to examine the effect of drugs at such a high dose in animal experiments. Fifth, plasma KP-10 concentration in ApoE<sup>-/-</sup> mice infused with KP-10 was significantly higher by 3- to 4-fold (Table 1), which were not as high as we anticipated. KP-10 might therefore be metabolized, to some degree, in circulating blood.<sup>43</sup> Last, plasma KP-10 concentration in ApoE<sup>-/-</sup> mice infused with KP-10+P234 was higher compared with KP-10 alone (Table 2). Given that the amino-acid sequence of KP-10 is 70% identical to that of P234 (inactive form), the ELISA kit may detect P234 as KP-10 (possible cross-reaction).

In conclusion, our results indicate that KP-10 accelerates atherogenesis by enhancing the inflammatory responses and monocyte adhesion in ECs and macrophage foam cell formation. In addition, KP-10 may contribute to plaque instability by reducing the proliferation of ECs and VSMCs and by increasing apoptosis and MMPs activities in VSMCs.

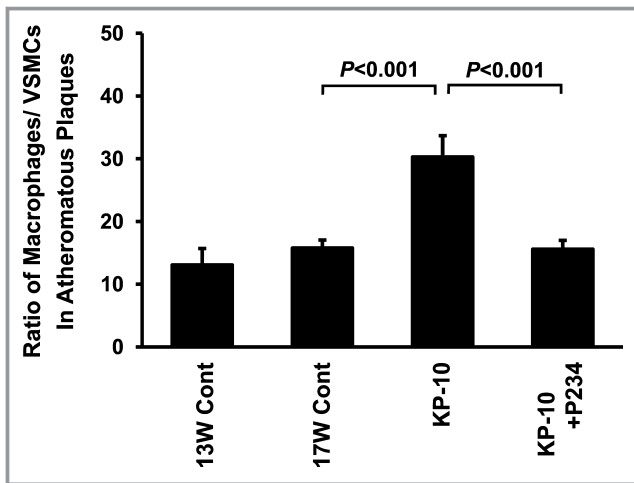


**Figure 7.** Effects of KP-10 and P234 (GPR54 antagonist) on atheromatous plaque instability in ApoE<sup>-/-</sup> mice. In experiment 2 shown in Figure 5, the ratio of macrophage content (µm<sup>2</sup>)/VSMC content (µm<sup>2</sup>) within atheromatous plaques was compared among 4 groups of 13-week-old mice (n=7) and 17-week-old mice infused with saline (n=10), KP-10 (12.5 µg/kg per hour; n=10), and KP-10 (12.5 µg/kg per hour)+P234 (50 µg/kg per hour) (n=11). KP-10 induces kisspeptin-10; VSMC, vascular smooth muscle cell.

The GPR54 antagonist may be useful for the prevention and treatment of atherosclerosis. Thus, the KP-10/GPR54 system may serve as a novel therapeutic target for atherosclerotic cardiovascular diseases.

## Acknowledgments

We thank Dr Fumiko Itoh for her helpful comments and Kaho Watanabe-Kominato, Maho Yamaguchi, Azumi Watanabe, and Hiroko Takeuchi for their technical assistances.

## Sources of Funding

This work was supported, in part, by a Grant-in-Aid for Young Scientists (B) (25860418 to Sato) and a Grant-in-Aid for Scientific Research (C) (16K08943 to Sato) from the Japan Society for the Promotion of Science.

## Disclosures

None.

## References

1. Ohtaki T, Shintani Y, Honda S, Matsumoto H, Hori A, Kanehashi K, Terao Y, Kumano S, Takatsu Y, Masuda Y, Ishibashi Y, Watanabe T, Asada M, Yamada T, Suenaga M, Kitada C, Usuki S, Kurokawa T, Onda H, Nishimura O, Fujino M. Metastasis suppressor gene KISS-1 encodes peptide ligand of a G-protein-coupled receptor. *Nature*. 2001;411:613–617.
2. Li D, Yu W, Liu M. Regulation of KISS1 gene expression. *Peptides*. 2009;30:130–138.
3. Kotani M, Dethoux M, Vandenbogaerde A, Communi D, Vanderwinden JM, Le Poul E, Brézillon S, Tyldesley R, Suarez-Huerta N, Vandeput F, Blanpain C, Schifmann SN, Vassart G, Parmentier M. The metastasis suppressor gene KISS-1 encodes kisspeptins, the natural ligands of the orphan G protein-coupled receptor GPR54. *J Biol Chem*. 2001;276:34631–34636.
4. Muir AI, Chamberlain L, Elshourbagy NA, Michalovich D, Moore DJ, Calamari A, Szekeres PG, Sarau HM, Chambers JK, Murdock P, Steplewski K, Shabon U, Miller JE, Middleton SE, Darker JG, Larminie CG, Wilson S, Bergsma DJ, Emson P, Faull R, Philpott KL, Harrison DC. AXOR12, a novel human G protein-coupled receptor, activated by the peptide KISS-1. *J Biol Chem*. 2001;276:28969–28975.
5. Lee JH, Miele ME, Hicks DJ, Phillips KK, Trent JM, Weissman BE, Welch DR. KISS-1, a novel human malignant melanoma metastasis-suppressor gene. *J Natl Cancer Inst*. 1996;88:1731–1737.
6. Lee JH, Welch DR. Identification of highly expressed genes in metastasis-suppressed chromosome 6/human malignant melanoma hybrid cells using subtractive hybridization and differential display. *Int J Cancer*. 1997;71:1035–1044.
7. Cho SG, Li D, Stafford LJ, Luo J, Rodriguez-Villanueva M, Wang Y, Liu M. KiSS1 suppresses TNF $\alpha$ -induced breast cancer cell invasion via an inhibition of RhoA-mediated NF- $\kappa$ B activation. *J Cell Biochem*. 2009;107:1139–1149.
8. Bilban M, Ghaffari-Tabrizi N, Hintermann E, Bauer S, Molzer S, Zoratti C, Malli R, Sharabi A, Hiden U, Graier W, Knöfler M, Andrae F, Wagner O, Quaranta V, Desoye G. Kisspeptin-10, a KISS-1/metastin-derived decapeptide, is a physiological invasion inhibitor of primary human trophoblasts. *J Cell Sci*. 2004;117:1319–1328.
9. Stafford LJ, Xia C, Ma W, Cai Y, Liu M. Identification and characterization of mouse metastasis-suppressor KISS1 and its G-protein-coupled receptor. *Cancer Res*. 2002;62:5399–5404.
10. Li XF, Kinsey-Jones JS, Cheng Y, Knox AM, Lin Y, Petrou NA, Roseweir A, Lightman SL, Milligan SR, Millar RP, O'Byrne KT. Kisspeptin signaling in the hypothalamic arcuate nucleus regulates GnRH pulse generator frequency in the rat. *PLoS One*. 2009;4:e8334.
11. Mead EJ, Maguire JJ, Kuc RE, Davenport AP. Kisspeptins are novel potent vasoconstrictors in humans, with a discrete localization of their receptor, G

- protein-coupled receptor 54, to atherosclerosis-prone vessels. *Endocrinology*. 2007;148:140–147.
12. Maguire JJ, Kirby HR, Mead EJ, Kuc RE, d'Anglemont de Tassigny X, Colledge WH, Davenport AP. Inotropic action of the puberty hormone kisspeptin in rat, mouse and human: cardiovascular distribution and characteristics of the kisspeptin receptor. *PLoS One*. 2011;6:e27601.
13. Sawyer I, Smillie SJ, Bodkin JV, Fernandes E, O'Byrne KT, Brain SD. The vasoactive potential of kisspeptin-10 in the peripheral vasculature. *PLoS One*. 2011;6:e14671.
14. Qureshi IZ, Kanwal S. Novel role of puberty onset protein kisspeptin as an anticoagulation peptide. *Blood Coagul Fibrinolysis*. 2011;22:40–49.
15. Cho SG, Yi Z, Pang X, Yi T, Wang Y, Luo J, Wu Z, Li D, Liu M. Kisspeptin-10, a KISS1-derived decapeptide, inhibits tumor angiogenesis by suppressing Sp-1-mediated VEGF expression and FAK/Rho GTPase activation. *Cancer Res*. 2009;69:7062–7070.
16. Ramaesh T, Logie JJ, Roseweir AK, Millar RP, Walker BR, Hadoke PW, Reynolds RM. Kisspeptin-10 inhibits angiogenesis in human placental vessels ex vivo and endothelial cells in vitro. *Endocrinology*. 2010;151:5927–5934.
17. Usui S, Iso Y, Sasai M, Mizukami T, Mori H, Watanabe T, Shioda S, Suzuki H. Kisspeptin-10 induces endothelial cellular senescence and impaired endothelial cell growth. *Clin Sci (Lond)*. 2014;127:47–55.
18. Matjila M, Millar R, van der Spuy Z, Katz A. Elevated placental expression at the maternal-fetal interface but diminished maternal circulatory kisspeptin in preeclamptic pregnancies. *Pregnancy Hypertens*. 2016;6:79–87.
19. Konii H, Sato K, Kikuchi S, Okiyama H, Watanabe R, Hasegawa A, Yamamoto K, Itoh F, Hirano T, Watanabe T. Stimulatory effects of cardiostrophin 1 on atherosclerosis. *Hypertension*. 2013;62:942–950.
20. Watanabe K, Watanabe R, Konii H, Shirai R, Sato K, Matsuyama TA, Ishibashi-Ueda H, Koba S, Kobayashi Y, Hirano T, Watanabe T. Counteractive effects of omentin-1 against atherogenesis. *Cardiovasc Res*. 2016;110:118–128.
21. Watanabe R, Watanabe H, Takahashi Y, Kojima M, Konii H, Watanabe K, Shirai R, Sato K, Matsuyama T, Ishibashi-Ueda H, Iso Y, Koba S, Kobayashi Y, Hirano T, Watanabe T. Atheroprotective effects of tumor necrosis factor-stimulated gene-6. *JACC Basic Transl Sci*. 2016;1:496–509.
22. Hasegawa A, Sato K, Shirai R, Watanabe R, Yamamoto K, Watanabe K, Nohtomi K, Hirano T, Watanabe T. Vasoprotective effects of urocortin 1 against atherosclerosis in vitro and in vivo. *PLoS One*. 2014;9:e0110866.
23. Naito C, Hashimoto M, Watanabe K, Shirai R, Takahashi Y, Kojima M, Watanabe R, Sato K, Iso Y, Matsuyama T, Suzuki H, Ishibashi-Ueda H, Watanabe T. Facilitatory effects of fetuin-A on atherosclerosis. *Atherosclerosis*. 2016;246:344–351.
24. Nagashima M, Watanabe T, Shichiri M, Sato K, Shirai R, Morita R, Terasaki M, Arita S, Hongo S, Miyazaki A, Hirano T. Chronic infusion of salusin- $\alpha$  and - $\beta$  exerts opposite effects on macrophage foam cell formation and atherosclerosis in apolipoprotein E-deficient mice. *Atherosclerosis*. 2010;212:70–77.
25. Roseweir AK, Kauffman AS, Smith JT, Guerriero KA, Morgan K, Pielecka-Fortuna J, Pineda R, Gottsch ML, Tena-Sempere M, Moenter SM, Terasawa E, Clarke IJ, Steiner RA, Millar RP. Discovery of potent kisspeptin antagonists delineate physiological mechanisms of gonadotropin regulation. *J Neurosci*. 2009;29:3920–3929.
26. de Roux N, Genin E, Carel JC, Matsuda F, Chaussain JL, Milgrom E. Hypogonadotropic hypogonadism due to loss of function of the KISS1-derived peptide receptor GPR54. *Proc Natl Acad Sci USA*. 2003;100:10972.
27. Merhi Z, Thornton K, Bonney E, Cipolla MJ, Charron MJ, Buyuk E. Ovarian kisspeptin expression is related to age and to monocyte chemoattractant protein-1. *J Assist Reprod Genet*. 2016;33:535–543.
28. Seminara SB, Messenger S, Chatzidakis EE, Thresher RR, Acierno JS Jr, Shagoury JK, Bo-Abbas Y, Kuohung W, Schwinf KM, Hendrick AG, Zahn D, Dixon J, Kaiser UB, Slaughaupt SA, Gusella JF, O'Rahilly S, Carlton MB, Crowley WF Jr, Aparicio SA, Colledge WH. The GPR54 gene as a regulation of puberty. *N Engl J Med*. 2003;349:1614–1627.
29. Clarkson J, Tassigny XA, Moreno AS, Colledge WH, Herbison AE. Kisspeptin-GPR54 signaling is essential for preovulatory gonadotropin-releasing hormone neuron activation and the luteinizing hormone surge. *J Neurosci*. 2008;28:8691–8697.
30. Bowe JE, King AJ, Kinsey-Jones JS, Foot VL, Li XF, O'Byrne KT, Persaud SJ, Jones PM. Kisspeptin stimulation of insulin secretion: mechanisms of action in mouse islets and rats. *Diabetologia*. 2009;52:855–862.
31. Tolson KP, Garcia C, Yen S, Simonds S, Stefanidis A, Lawrence A, Smith JT, Kauffman AS. Impaired kisspeptin signaling decreases metabolism and promotes glucose intolerance and obesity. *J Clin Invest*. 2014;124:3075–3079.
32. Mezei Z, Zamani-Forooshani O, Csabafi K, Szikszai B, Papp E, Ónodi Á, Török D, Leprán Á, Telegdy G, Szabó G. The effect of kisspeptin on the regulation of vascular tone. *Can J Physiol Pharmacol*. 2015;93:787–791.

33. Guo P, Zhang SZ, He H, Zhu YT, Tseng SC. PTX3 controls activation of matrix metalloproteinase 1 and apoptosis in conjunctivochalasis fibroblasts. *Invest Ophthalmol Vis Sci.* 2012;53:3414–3423.
34. Guo T, Ke L, Qi B, Wan J, Ge J, Bai L, Cheng B. PTX3 is located at the membrane of late apoptotic macrophages and mediates the phagocytosis of macrophages. *J Clin Immunol.* 2012;32:330–339.
35. Klouche M, Peri G, Knabbe C, Eckstein HH, Schmid FX, Schmitz G, Mantovani A. Modified atherogenic lipoproteins induce expression of pentraxin-3 by human vascular smooth muscle cells. *Atherosclerosis.* 2004;175:221–228.
36. Shindo A, Tanemura H, Yata K, Hamada K, Shibata M, Umeda Y, Asakura F, Toma N, Sakaida H, Fujisawa T, Taki W, Tomimoto H. Inflammatory biomarkers in atherosclerosis: pentraxin 3 can become a novel marker of plaque vulnerability. *PLoS One.* 2014;9:e100045.
37. Yoshioka K, Ohno Y, Horiguchi Y, Ozu C, Namiki K, Tachibana M. Effects of a KiSS-1 peptide, a metastasis suppressor gene, on the invasive ability of renal cell carcinoma cells through a modulation of a matrix metalloproteinase 2 expression. *Life Sci.* 2008;83:332–338.
38. Yan C, Wang H, Boyd DD. KiSS-1 represses 92-kDa type IV collagenase expression by down-regulating NF- $\kappa$ B binding to the promoter as a consequence of I $\kappa$ B $\alpha$ -induced block of p65/p50 nuclear translocation. *J Biol Chem.* 2001;276:1164–1172.
39. Claise C, Edeas M, Chaouchi N, Chalas J, Capel L, Kalimoutou S, Vazquez A, Lindenbaum A. Oxidized-LDL induce apoptosis in HUVEC but not in the endothelial cell line EA.hy 926. *Atherosclerosis.* 1999;147:95–104.
40. Olszanecki R, Gebeska A, Korbut R. Production of prostacyclin and prostaglandin E2 in resting and IL-1 $\beta$ -stimulated A549, HUVEC and hybrid EA.hy926 cells. *J Physiol Pharmacol.* 2006;57:649–660.
41. Nijher GM, Chaudhri OB, Ramachandran R, Murphy KG, Zac-Varghese SE, Fowler A, Chinthapalli K, Patterson M, Thompson EL, Williamson C, Kumar S, Ghatei MA, Bloom SR, Dhillon WS. The effects of kisspeptin-54 on blood pressure in humans and plasma kisspeptin concentrations in hypertensive diseases of pregnancy. *Br J Clin Pharmacol.* 2010;70:674–681.
42. Jayasena CN, Abbara A, Narayanaswamy S, Comninou AN, Ratnasabapathy R, Bassett P, Mogford JT, Malik Z, Calley J, Ghatei MA, Bloom SR, Dhillon WS. Direct comparison of the effects of intravenous kisspeptin-10, kisspeptin-54 and GnRH on gonadotrophin secretion in healthy men. *Hum Reprod.* 2015;30:1934–1941.
43. Liu Z, Ren C, Jones W, Chen P, Seminara SB, Chan YM, Smith NF, Covey JM, Wang J, Chan KK. LC-MS/MS quantification of a neuropeptide fragment kisspeptin-10 (NSC 741805) and characterization of its decomposition product and pharmacokinetics in rats. *J Chromatogr B Analyt Technol Biomed Life Sci.* 2013;926:1–8.

# **SUPPLEMENTAL MATERIAL**

## **Data S1**

### **Supplemental Methods**

#### **Human Sample Collection in Patients With Coronary Artery Disease (CAD)**

This study was received prior approval from the Ethics Committees of Showa University and Tokyo University of Pharmacy and Life Sciences. Informed consent was obtained from a total of 98 participants prior to their enrollment. Blood was drawn from 70 patients with acute coronary syndrome (ACS), admitted within 4 hours after onset to Showa University Hospital for emergency coronary catheterization (42 men, 28 women; aged 22–88); 28 healthy volunteers (17 men, 11 women; aged 21–56) were also recruited. ACS patients included 53 with acute myocardial infarction and 17 with unstable angina pectoris. Plasma KP-10 level was measured by enzyme-linked immunosorbent assay (ELISA; Phoenix Pharmaceuticals) after extraction with Sep-Pak C18 cartridge (Waters Associates) as described before.<sup>1</sup>

Buffered 10% formalin-fixed paraffin-embedded human coronary artery specimens from archive collections of the National Cerebral and Cardiovascular Center were used for immunohistochemistry. Serial cross-sections (3–4  $\mu\text{m}$ ) of coronary arteries from 14 patients with CAD (aged 60–87) and 4 patients with dilated cardiomyopathy (as non-CAD examples) (aged 19–39) were stained with polyclonal rabbit antibody against human KP-10 or its receptor GPR54 (LifeSpan BioSciences) as described previously.<sup>2,3</sup>

### **Supplemental Results**



## **Expressions of KP-10 and GPR54 in Coronary Artery Lesions and Plasma in CAD**

### **Patients**

Faint expressions of KP-10 and GPR54 were observed in the endothelium of normal coronary arteries from non-CAD patients (Figure S2A: a, b). KP-10 also was abundantly expressed in adventitia (Figure S2A: a). In stenotic and obstructive coronary arteries from CAD patients, both KP-10 and GPR54 were expressed at high levels in the atheromatous plaques (Figure S2A: c–h). Both KP-10 and GPR54 expressions became greater in accordance with the severity of atheromatous plaques (Figure S2A: c–h). In contrast, plasma KP-10 level tended to be reduced in CAD (ACS) patients compared with healthy volunteers (Figure S2B). We speculate that plasma KP-10 may be rapidly exhausted in thrombus formation in the coronary arteries within 4 hours after onset of ACS, because KP-10 is also known to act as an anti-coagulant and thrombolytic agent.<sup>4</sup>

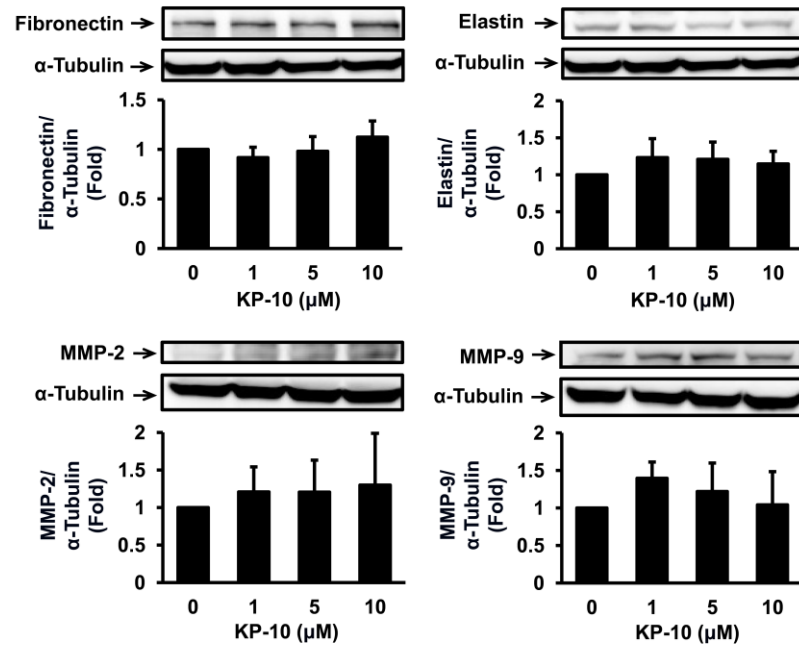
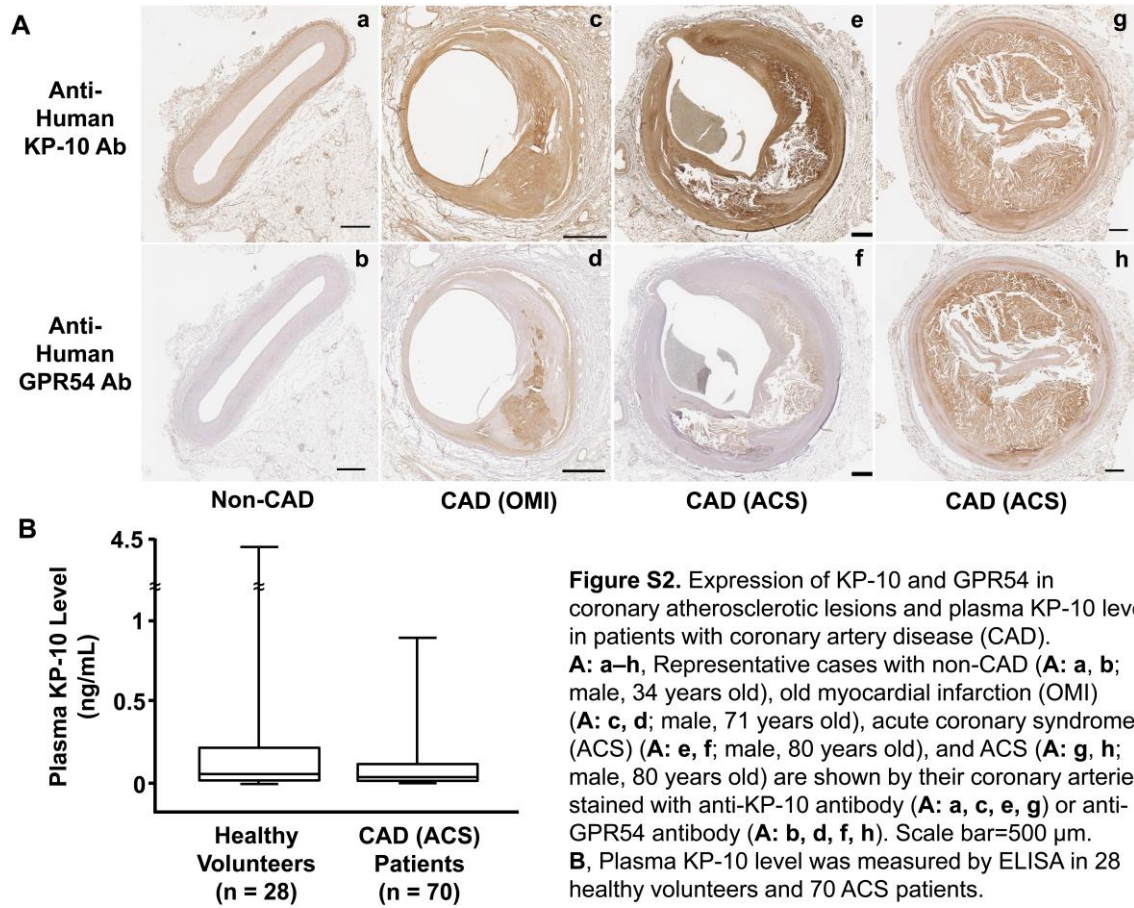


**Figure S1.** Effects of KP-10 on extracellular matrix expression in human aortic smooth muscle cells (HASMCs). HASMCs were incubated with the indicated concentrations of KP-10 for 24 hours and subjected for immunoblot analyses of fibronectin, elastin, metalloproteinase (MMP)-2, and MMP-9. Representative images showing protein expression (upper panels) with densitometry following normalization relative to  $\alpha$ -tubulin (lower panels). Data are shown as means  $\pm$  SEM from 4 independent experiments.



### Supplemental References:

1. Sato K, Koyama T, Tateno T, Hirata Y, Shichiri M. Presence of immunoreactive salusin- $\alpha$  in human serum and urine. *Peptides*. 2006;27:2561–2566.
2. Watanabe K, Watanabe R, Konii H, Shirai R, Sato K, Matsuyama TA, Ishibashi-Ueda H, Koba S, Kobayashi Y, Hirano T, Watanabe T. Counteractive effects of omentin-1 against atherogenesis. *Cardiovasc Res*. 2016;110:118–128.
3. Watanabe R, Watanabe H, Takahashi Y, Kojima M, Konii H, Watanabe K, Shirai R, Sato K, Matsuyama T, Ishibashi-Ueda H, Iso Y, Koba S, Kobayashi Y, Hirano T, Watanabe T. Atheroprotective Effects of Tumor Necrosis Factor-Stimulated Gene-6. *JACC Basic Transl Sci*. 2016;1:496–509.
4. Qureshi IZ, Kanwal S. Novel role of puberty onset protein kisspeptin as an anticoagulation peptide. *Blood Coagul Fibrinolysis*. 2011;22:40–49.